Soft Matter

Accepted Manuscript

ROYAL SOCIETY
OF CHEMISTRY

www.rsc.org/softmatter

ARTICLE TYPE

Dynamic self-assembly of colloids through periodic variation of inter-particle potentials

Sumedh R. Risbud and James W. Swan[*]

A short-ranged and time-varying attraction drives self-assembly of colloidal crystals from a suspension of colloidal spheres. Brownian Dynamics simulations of this process demonstrate that the envelope for self-assembly of large, low defect crystals is broadened dramatically when this attractive interaction is switched on and off periodically in time. This process is termed dynamic self-assembly because temporal control of the inter-particle potential requires injection and extraction of energy from the self-assembling materials. We develop a theory using non-equilibrium statistical mechanics to determine the rate at which particles cross a similarly switched energy barrier, and show that there is a switching rate that maximizes barrier crossing. While barrier crossing towards thermodynamic equilibrium is limited by the Kramers hopping rate, the rate of out-of-equilibrium barrier crossing can exceed this limit. In the context of self-assembly, barrier crossing is the rate limiting step and responsible for both defect formation and slow nucleation. This simple theory is used to explain the optimal switching rate observed in our simulations of dynamic self-assembly. Dynamic self-assembly via switched potentials enables growth of ordered phases without thermodynamic constraints on the assembly kinetics.

1 Introduction

Spatially ordered structures comprising arrays of micro- and nano-particles are the basis of many cutting edge technologies applied to solar energy harvesting,[1] energy storage,[2,3] biological and chemical sensors,[4] electronic applications including 3D photonic crystals,[5] low-power displays,[6] bioelectronic devices,[7] and high performance thermal insulators[8]. Although the raw materials required for manufacturing ordered arrays of colloids are relatively inexpensive, a consistent, cost-effective protocol for large scale fabrication of low defect structures with high production rate has remained elusive.

Thermodynamic self-assembly (crystallization close to equilibrium) is the principal method for laboratory-scale fabrication of ordered colloidal phases.[9] Usually aggregation is driven by a carefully engineered steady attraction between suspended particles. This interaction leads to nucleation and growth of an ordered phase.[10,11] The strength of the attraction must be chosen such that nucleation of crystals is a rare event. Otherwise ordered phases with high defect density are produced. The process of aggregation and growth is passive, and there exists a narrow range of operating conditions under which low defect crystals can be grown. The potential energy landscape associated with this self-assembly process is typically rough – presenting kinetic barriers and numerous lo-

cal minima associated with meta-stable states such as glasses, gels, and fluids.[12]

Consequently, dilute suspensions subjected to strong attractive potentials or concentrated suspensions in relatively weak potentials must be self-assembled near the boundary for phase separation. Although high quality and defect-free crystal domains can be obtained under such conditions. The time scales associated with nucleation and growth, are governed by slow kinetics associated with Kramers hopping. Thermal fluctuations must give rise to a crystal nucleus with sufficient size to grow continuously. This nucleus size can be predicted by the classical nucleation theory (CNT), and the time scales associated with observation of such a fluctuation are necessarily long to ensure low defect rates.[13,14] Moreover, nucleation rates are known to be very sensitive to operating conditions, for example, even a 3% variation in particle concentration decreases the nucleation rate by a factor of 10^5 in the self-assembly of colloidal hard-spheres.[15]

Suspensions with strong attractive interactions are driven to quickly phase separate due to spinodal decomposition. Here, a single particle can serve as a critical nucleus and growth of the ordered phase is spontaneous.[13] Despite the speed of this process, the end product is usually kinetically arrested with the condensed phase dominated by meta-stable glassy, jammed, or gel-like structures. These meta-stable states relax with Kramers hopping kinetics as well. Thus, purely thermodynamic constraints dictate the kinetics (and hence feasibility) of traditional approaches to self-assembly.

Department of Chemical Engineering, Massachusetts Institute of Technology, Cambridge MA 02139, USA.
[*] Tel: +1 (617) 324-7359; E-mail: jswan@mit.edu

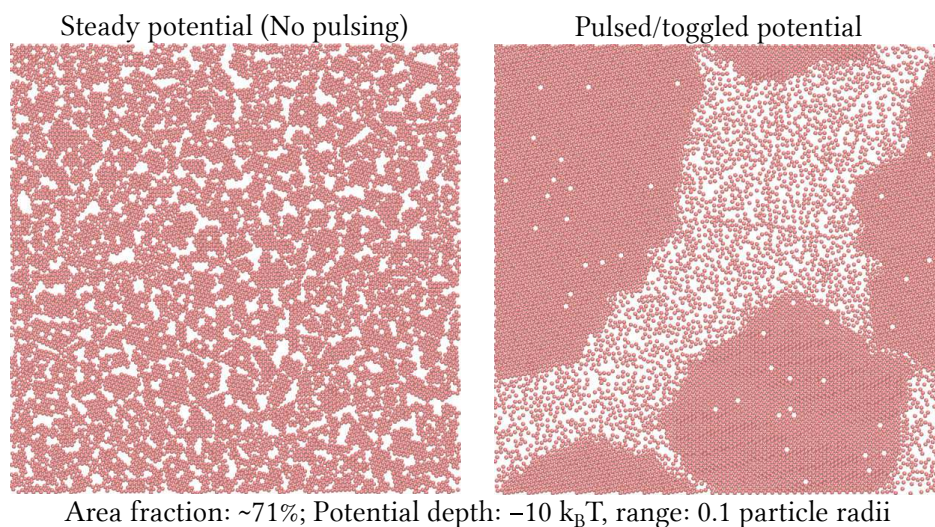Area fraction: ~71%; Potential depth: −10 $k_B T$, range: 0.1 particle radii

Fig. 1 For the same concentration and short-range attractive potential, a steady potential leads to a kinetically arrested glass (Left) while a pulsed potential leads to low defect crystal coexisting in steady state with a fluid (Right). In both cases depicted above, the systems were simulated for 3000 diffusion times (1 diffusion time = 1 a^2/D, where $a \equiv$ particle radius and $D \equiv$ particle self-diffusivity). (Right) The potential was pulsed at a frequency of 100 D/a^2 and a duty cycle of 1, i.e., total 300000 equal duration on-off periods were simulated.

Recently, experiments by Swan and co-workers have shown that exposing a suspension of paramagnetic colloidal particles to a periodically switched magnetic field enables the suspension to overcome these thermodynamically imposed kinetic constraints. They showed that simple time variation of the inter-particle attraction can speed up the self-assembly process by several orders of magnitude.[16,17] This strategy is called *dynamic* self-assembly, owing to its inherent out-of-equilibrium nature. The experiments further reveal that there exists an *optimal* switching rate at which the suspension finds the crystalline state fastest.[17] It was postulated that dynamic self-assembly lowers the kinetic barriers by allowing the particles to relax diffusively during the portion of the cycle in which the magnetic field is switched off.[16,17] This process is akin to annealing of crystals by raising and lowering temperature. However, the optimal switching rate was found to be proportional to the characteristic diffusion rate of the paramagnetic particles.

In this article, we investigate dynamic self-assembly of suspensions in two dimensions via Brownian dynamics simulations. The particles in a suspension of hard-spheres are subjected to a periodically-pulsed, short-range, attractive potential. Fig. 1 depicts the result of two simulations: the control case in which the switching rate is zero (the attractive potential is steady), and a case in which the potential is switched. The simulations reveal that, for the same depth and range of the potential, a steady attraction yields glassy, kinetically arrested structures while an optimally pulsed time-periodic potential leads to a low defect crystalline state (see Fig. 1). The dy-

namic variables associated with the pulsing process are: the duration of the off portion of the pulse, the ratio of on-to-off durations of the pulsing cycle called the duty cycle, and the concentration of the suspension. In Section 2, we present the methodology adopted for the Brownian dynamics simulations. We observe, as in the case of experiments, that there exists an optimal off-period which leads to fastest nucleation and growth of crystalline domains (Section 3.1). In section 3.2 we develop a simple theory for the rate at which particles cross a pulsed energy barrier. We use this theory and the simulation results to validate a hypothesis that the optimal off-period corresponds to the rate of inter-particle diffusion over the range of the applied potential. This relationship can be rationalized by recognizing that the defects characteristic of kinetic arrest can be annealed by relatively small particle displacements. Allowing the particles to periodically diffuse freely to the outer limit of the inter-particle potential creates opportunities for local configurations of particle to find better ordered states without barrier crossing. This was postulated in the context of experiments by Swan and co-workers, where the 'capture radius' of a magnetically induced inter-particle potential was used to identify optimal conditions for dynamic self-assembly of suspensions of paramagnetic colloids.[17] In Section 3.3, we study how the duty cycle of the optimally pulsed potential affects the self-assembly process and show that duty cycle is critical for controlling the rate of crystal nucleation in dynamic self-assembly.
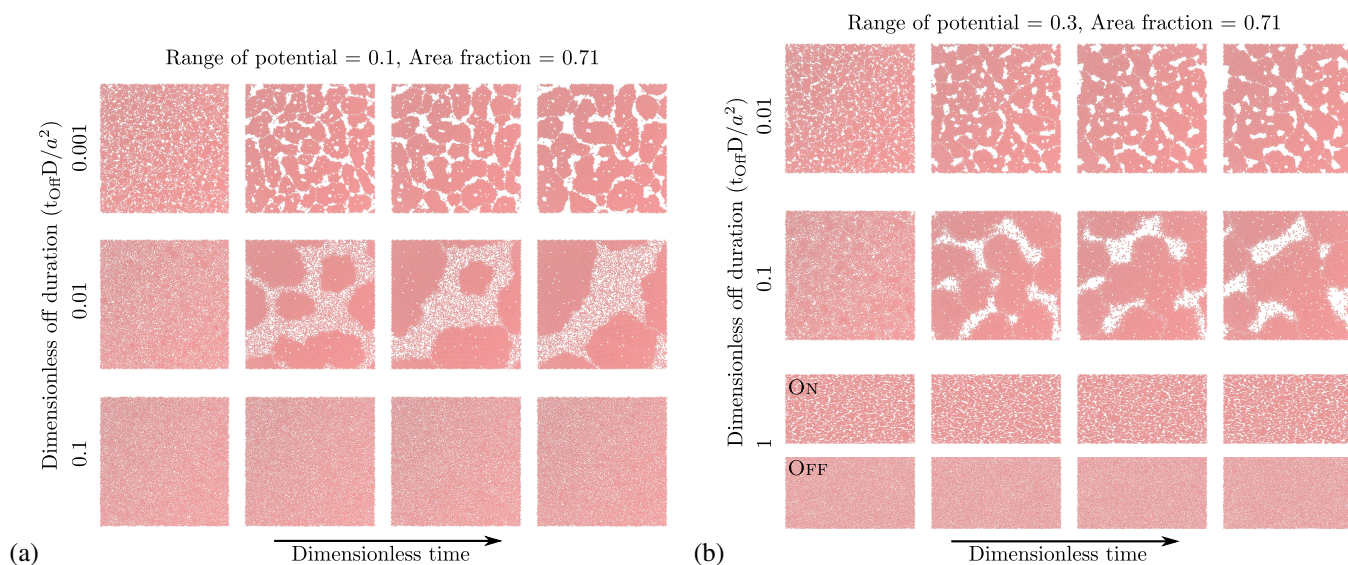
Fig. 2 Subfigures (a) & (b) show time-lapsed snapshots of 2 sets of simulations corresponding to different ranges of inter-particle pair potential, respectively. Both show temporal evolution of suspension microstructure for a duty cycle of $\eta = 1$ and three different off durations (i.e., t_{Off}): optimal (middle row), an order of magnitude shorter than optimal (top row), and an order of magnitude longer than optimal (top row). We observe that pulsing the potential with t_{Off} shorter than its optimal value leads to a glassy self-assembly. On the other hand, no nucleation is observed if t_{Off} is longer than the optimal. The bottom row of (b) consists of two sub-rows that depict the suspension structure during on state (glassy and arrested) and off state (thermalized fluid) of pulsing cycle ($t_{Off} = 1 \ a^2/D$). The off duration in this case is sufficiently long to dissolve any structure formed during the on duration entirely.

2 Methodology

In this work, we perform Brownian dynamics (BD) simulations of hard spheres constrained to a plane using the HOOMD simulation suite (Highly Optimized Object-oriented Many-particle Dynamics).[18] We simulate $N_p = 10000$ identical particles of unit radius ($a = 1$) in an $L \times L$ simulation box; the latter is chosen to attain a given area concentration ($\phi = N_p \pi a^2 / L^2$). The concentrations examined in this work are $\phi = 0.15, 0.20, 0.26, 0.35, 0.46, 0.59, 0.65,$ and 0.71. All particles have unit drag coefficients ($\gamma = 1$). Time is measured in the units of diffusion timescale of a single particle a^2/D, where, diffusivity is given by, $D = k_B T / \gamma$ (consequently, frequencies are measured in the units of D/a^2).

Under experimental conditions, since the system under consideration is planar, the particle motion is expected to be in close proximity of a fixed wall. A wall will screen hydrodynamic interactions between the particles, and the chief role of hydrodynamics will be to slow the motion of the particles.[19–21] In lieu of modeling such interactions, which can be quite costly computationally, we neglect the effect of interparticle hydrodynamic interactions; it is an assumption typically tacit in Brownian dynamics simulations.

The motion of colloidal scale particles is overdamped. This implies that the timescale associated with inertial relaxation

is negligible. This renders the mass of the particles irrelevant. HOOMD uses velocity-Verlet (two-step) algorithm to integrate Newton's equations of motion for the particles. As shown in Appendix A, in the velocity-Verlet integration scheme, if the particle mass is set to the product of its drag coefficient and the time-step, the integration scheme simplifies to forward-in-time Euler integration of the exact overdamped dynamics of a colloid, with negligible inertia. Therefore, with this choice of mass, overdamped dynamics of colloidal particles can be simulated using a traditional MD integrator by setting particle mass proportional to the time-step.

Two different pair potentials are employed in the simulations: a hard-sphere potential (HP) which is not a function of time and acts only if particles overlap during the course of a simulation, and a temporally periodic, attractive, switched potential (SP). The HP is modeled as a Hookean spring,

$$U_H(r) = \frac{\gamma}{4\Delta t} (r - 2a)^2 H(2a - r),$$

where r is the separation between particle centers and H is the Heaviside step function. Due to the peculiar dependence of the spring constant: $\gamma/(2\Delta t)$, on time-step and drag coefficient, the relative displacement caused by the force due to the HP is exactly $(2a - r)\hat{\mathbf{r}}$. Thus, the HP generates displacements that exactly resolve the overlaps between touching particle pairs.[22]

Observe that the potential U_H is depends only on particle properties (drag and radius) and adapts to the choice of time-step. It represents a generic and parameter-free repulsion between particles, capturing the effect of short-ranged repulsions like double-layer, surface roughness, etc.[23] Thus, we choose it as a representative functional form for inter-particle repulsion.

For particles of unit radius ($a = 1$), the switched potential (between on and off states) is given as,

$$U_S(r) = \frac{\varepsilon (1+\delta_0)^3}{\delta_0^2 \left(\frac{3}{2}+\delta_0\right)} \times$$
$$\left[1 - \frac{3}{2}\frac{r}{2(1+\delta_0)} + \frac{1}{2}\left(\frac{r}{2(1+\delta_0)}\right)^3\right] \times$$
$$[H(r-2) - H(r-2(1+\delta_0))],$$

where ε characterizes the depth of the potential and δ_0 quantifies its dimensionless range. This is a depletion potential, and throughout this work, we have set $\varepsilon = -10k_BT$ when attractions are on and $\varepsilon = 0k_BT$ when attractions are off. Two attraction ranges are studied: $\delta_0 = 0.1$ and 0.3. Three durations over which the potential is off, t_{off} are studied in detail for each range of attraction:

δ_0	t_{off}
0.1	0.1, 0.01, 0.001
0.3	1, 0.1, 0.01

It has been shown that the reduced second virial coefficient of a colloidal 'sticky' hard-sphere-system is insensitive to the specific choice of the attractive potential.[24] Thus, the particular functional form for the inter-particle attraction (i.e., the Asakura-Oosawa depletion potential in this case) should be understood as a representative short-ranged pairwise attractive potential.

The duty cycle ($\eta = t_{on}/t_{off}$) of the switched potential is the ratio of the duration on to the duration off. The effect of duty cycle on the crystallization kinetics, is investigated by examining the following duty cycle-area fraction doublets with $t_{off} = 0.01$ and $\delta_0 = 0.1$:

η	ϕ
0.5	0.59, 0.65, 0.71
1	0.52, 0.59, 0.65, 0.71
1.5	0.52
2	0.35, 0.46, 0.52, 0.59, 0.65, 0.71
3	0.20, 0.26, 0.35, 0.46, 0.59, 0.65, 0.71
4	0.15, 0.20, 0.26, 0.35, 0.46
5	0.15, 0.20, 0.26
6	0.15

3 Results and discussions

3.1 Optimal off duration of a pulse: Brownian Dynamics

First, consider the case when the potential is pulsed with unit duty cycle, i.e., $\eta = 1$. The off duration is resposible for relaxation of the arrested structure and consequent annealing of defects via diffusion. At high pulsing frequencies, the off duration is short and a glassy particle cluster cannot rearrange effectively. In fact, at very high frequencies the pulsing process can be replaced by an *effective steady potential* given by the average of the on and off states over a pulsing cycle (see Appendix B). At sufficiently low frequencies, the off duration is long and crystalline domains formed during the on-state dissolve via diffusion. However, if the off duration is $\sim \delta_0^2 a^2/D$, the particles can diffuse a distance of the order of $\delta_0 a$ and locally glassy configurations have the opportunity to find a well-ordered state without barrier crossing. In other words, the optimal off duration for rapid self-assembly lies between the two extremes of fast and slow pulsing, and is similar in order of magnitude to the time required for diffusion of a single particle through the range of the potential.

For $\delta_0 = 0.1$ and 0.3, we expect to observe rapid self-assembly when $t_{off} \sim 0.1^2 a^2/D$ and $\sim 0.3^2 a^2/D$, respectively. Fig. 2 corroborates this prediction for a monolayer of Brownian spheres with 71% area fraction. Swan *et al.*[17] have experimentally verified a similar estimate for the specific case of magnetic field-driven assembly of paramagnetic colloids, wherein the range of the attractive potential is replaced by an effective 'capture radius'. However, this comparison is qualitative, as the inter-particle potential used by Swan and co-workers is long-ranged dipole-dipole magnetic interaction, which is 'directional' in nature as against the short-ranged radially isotropic potential employed in this work.

Further insight into the temporal evolution of the microstructure during the process of self-assembly can be gained by examining the evolution of the mean wave-number associated with the suspension microstructure $\langle q \rangle_1$. The mean wave-number is computed from the structure factor $S(q)$ as follows,[24]

$$\langle q \rangle_1 = \frac{\int_0^{q_c} q S(q)\mathrm{d}q}{\int_0^{q_c} S(q)\mathrm{d}q},$$

where $q_c = 3.0$ is used as a cutoff value. At $q_c = 3.0$, the corresponding length scale is $\sim 2\pi a/q_c \approx 2.1a$, which is of the order of one particle diameter. Thus, by definition, this mean wave-number captures the characteristic length scale of particle clusters larger than two particles in size. A temporally decreasing mean wave-number indicates that the characterisitic length scale increases with time. The particular nature of temporal dependence of the mean wave-number signifies the mode of aggregation followed by the particles, leading to a particular micro-structure. For example, in Fig. 3, the off
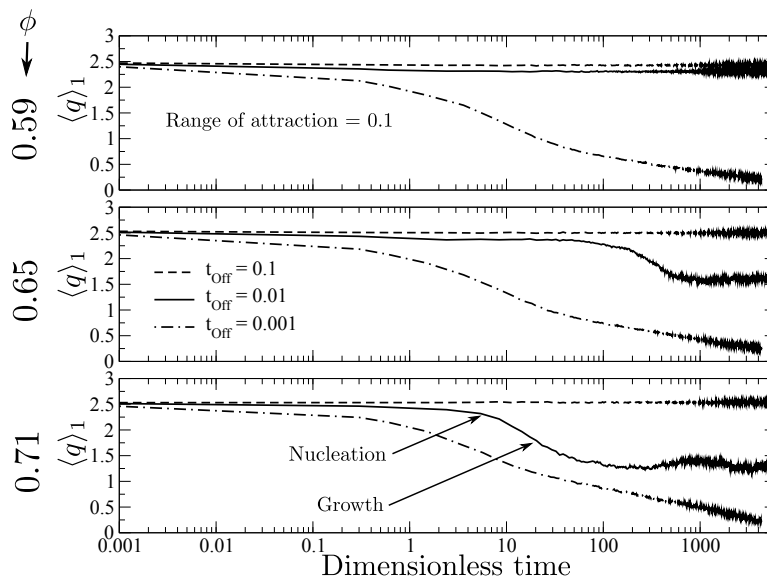
Fig. 3 Top, middle, and bottom panels portray the temporal evolution of mean wave number $\langle q \rangle_1$ for three concentrations, 59%, 65%, and 71%, respectively. The range of inter-particle pair potential is $\delta_0 = 0.1$ in all three cases. Each panel shows the evolution for three off durations: 0.1, 001, and 0.001, and a pulsing duty cycle $\eta = 1$. The dot-dashed curves corresponding to $t_{Off} = 0.001$ show a power law decay consistent with gelation for all three concentrations (see text). $t_{Off} = 0.01$ corresponds to the optimal off duration for $\delta_0 = 0.1$. Consequently, signatures of nucleation and growth can be seen in middle and bottom panels (concentrations of 65 and 71%). However, a concentration of 59% is to too dilute for nucleation to take place with a duty cycle of 1 (see Section 3.3).

duration of 0.01 is near-optimal for self-assembly and the corresponding $\langle q \rangle_1$ exhibits nucleation and growth events as indicated by a sudden decrease followed by stabilization to a steady state value, for $\phi = 0.65$ and 0.71. On the contrary, the most dilute suspension with $\phi = 0.59$ does not exhibit crystallization and remains in the colloidal 'fluid' state throughout the simulation. Furthermore, nucleation is delayed in the suspension with $\phi = 0.65$ and results in smaller crystalline domains compared to that with $\phi = 0.71$. The nucleation and growth processes depend on the concentration of the suspension and the duty cycle, which are discussed in Section 3.3.

In Fig. 2(a) (top row), when of $t_{Off} = 0.001$, we observe kinetically arrested, system-spanning, glassy structure without an inherent length scale. In Fig. 3, this lack of a characteristic length scale reflects as a power law dependence of $\langle q \rangle_1$ on time for the off duration 0.001, across all concentrations.[24] On the other hand, when the off duration is 0.1, the suspension remains a fluid with few density fluctuations, resulting in an almost constant $\langle q \rangle_1$.

3.2 Optimal off duration of a pulse: kinetic theory

So far, the existence of an optimal off duration for pulsing has been demostrated using scaling arguments and empirically, through Brownian dynamics simulations in the previous sec-
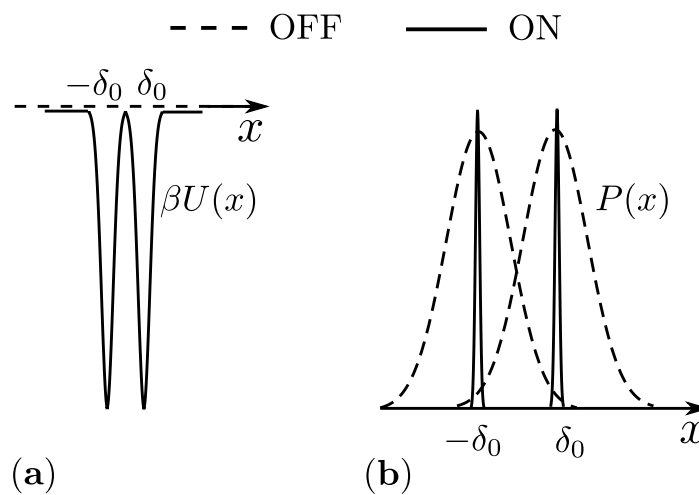

Fig. 4 A schematic representing (a) the potential energy landscape used to build a framework based on kinetic theory, and (b) the respective probability density functions.

tion and through experiments by Swan *et al.*[17] Although the problem is not amenable to a full theoretical treatment involving many-body interactions, a framework can be built in terms of a simple model with a unidimensional potential landscape and a population of otherwise non-interacting Brownian particles.

Suppose such a population of Brownian particles resides in an energy landscape that changes in time. The landscape is comprised by a potential with wells at $x = \pm\delta_0$ and a barrier between them at $x = 0$ that is turned on and off periodically in time (Fig. 4). The notation has been kept consistent in the context of our discussion in the previous section, and δ_0 signifies the range of the unidimensional potential. When the potential is off, the energy landscape is flat and the particles diffuse freely. When the potential is on, the particles are localized near $x = \pm\delta_0$ (see Fig. 4). Here, the two potential wells can be thought to signify two different phases (say, crystalline and glassy), and the coordinate parametrizing the unidimensional landscape can be thought of as an aproporiate order parameter.

The potential is assumed to be deep so that on time scales short relative to the Kramers mean first passage time, the particles are fixed exactly at $x = \pm\delta_0$. That is, their distribution is

$$\phi\delta(x - \delta_0) + (1 - \phi)\delta(x + \delta_0), \qquad (1)$$

where ϕ is the fraction of particles residing in the well at $x = \delta_0$, and $\delta(x)$ is the Dirac's δ-function (not to be confused with the range of the potential). In congruence with the assumption that the two potential wells signify two phases, henceforth the population in the well at $x = \delta_0$ is considered to be the 'favorable' population (say, crystalline phase in terms of the discussion in the previous section). Further, we require that all particles to the right of $x = 0$ just before the potential is turned on, go to the well at $x = \delta_0$.

An initial distribution of particles, $P_0(x)$ changes in time when the potential is switched from off to on state, and becomes:

$$P(x,t) = \delta(x - \delta_0)\int_0^\infty P_0(x)dx + \delta(x + \delta_0)\int_{-\infty}^0 P_0(x)dx, \quad (2)$$

because particles to the right of the barrier go to the well at $x = \delta_0$. The fraction of particles to the right of the barrier $(x > 0)$ is:

$$\phi = \int_0^\infty P_0(x)dx. \qquad (3)$$

Equivalently, if the initial distribution in the on state is $P_0(x)$, it evolves upon switching the potential off, under free diffusion, to become:

$$P(x,t) = \int_{-\infty}^\infty G(x - x', t)P_0(x')dx' \qquad (4)$$

where

$$G(x,t) = \frac{1}{\sqrt{4\pi Dt}}e^{-\frac{x^2}{4Dt}}, \qquad (5)$$

is the Green's function for diffusion in one dimension and D is the diffusivity.

Now, consider a pulsing process in which the potential energy landscape is pulsed between on and off with period T and duty cycle $\eta = 1$, i.e., $t_{Off} = T/2$. We assume that the period T is small compared to the Kramers mean first passage time corresponding to the unidimensional potential, and the flux across the barrier between the wells is negligible during the on part of the pulsing process.

If the landscape is toggled on at time $t = (n-1)T$, according to equation 2, the distribution of particles for $t > (n-1)T$ is given by,

$$P(x,t) = \phi(n)\delta(x - \delta_0) + (1 - \phi(n))\delta(x + \delta_0). \qquad (6)$$

Here, $\phi(n)$ is the population of particles to the right of the origin $(x > 0)$, at the end of the previous on-off pulse. Subsequently, using equation 4, the distribution after the landscape is toggled off at time $t = (n - 1/2)T$ is given by,

$$P(x,t) = \phi(n)G\left(x - \delta_0, \, t - \left(n - \frac{1}{2}\right)T\right)$$

$$+ (1 - \phi(n))G\left(x + \delta_0, \, t - \left(n - \frac{1}{2}\right)T\right), \qquad (7)$$

for times $t > (n - 1/2)T$. At the end of the nth pulse (at $t = nT$), the potential is toggled on again and the distribution of particles becomes:

$$P(x,t) = \phi(n+1)\delta(x - \delta_0) + (1 - \phi(n+1))\delta(x + \delta_0). \quad (8)$$

Therefore, using equations 3, 7, and 8:

$$\phi(n+1) = \int_0^\infty \left[\phi(n)G(x - \delta_0, T/2) \right.$$

$$\left. + (1 - \phi(n))G(x + \delta_0, T/2)\right]dx$$

$$= \frac{1}{2} + \text{erf}\left(\sqrt{\frac{\delta_0^2}{2DT}}\right)\left(\phi(n) - \frac{1}{2}\right). \qquad (9)$$

The above equation defines a recurrence relation for the fraction of particles to the right of the barrier $(x > 0)$ during the on duration of the potential. The solution of this recurrence relation is,

$$\phi(n) = \frac{1}{2} + \left[\text{erf}\left(\frac{1}{\sqrt{2\tau}}\right)\right]^n\left(\phi(0) - \frac{1}{2}\right) \qquad (10)$$

where the quantity $\tau = DT/\delta_0^2$ is the period of the on-off process made dimensionless on the time required for particles to diffuse freely through the range of the potential. Since τ is strictly positive, the nth power of the error function approaches
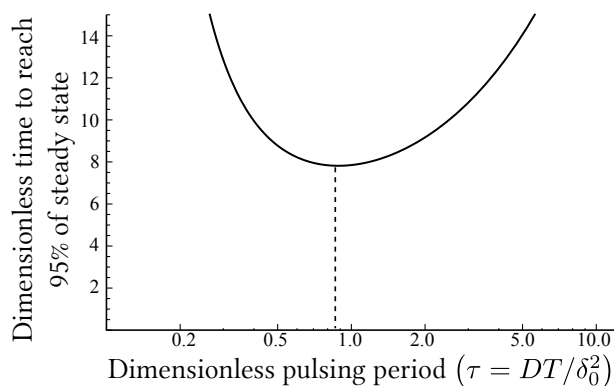
Fig. 5 The time required to achieve 95% conversion from an initial state with all the particles in the well at $x = \delta_0$ as a function of pulse period. The dashed line indicates the minimum at $\tau \approx 0.88$.

zero monotonically in n. Therefore, in this simple model, the steady state distribution ($n \to \infty$), yields half the particles to the right of the barrier.

The number of cycles n can be replaced by $n = t/\tau$ into equation 9, with t the elapsed time made dimensionless on the particle diffusion time. In terms of time t, the fraction of particles to the right of the barrier is:

$$\phi(t) = \frac{1}{2} + \left[\text{erf} \left(\frac{1}{\sqrt{2\tau}} \right) \right]^{t/\tau} \left(\phi(0) - \frac{1}{2} \right). \quad (11)$$

Noting that $\phi = 1/2$ at steady state, an optimality criterion for the pulsing process can be posed as: is there a value of τ for which $\phi(t)$ takes the least amount of time to attain steady state? Minimizing $(\phi(t) - 1/2)^2$ with respect to τ yields $\tau_{\text{opt}} \approx 0.88$, at which approach to the steady state is the fastest.

Equation 11 when rearranged gives the time t taken to attain a fixed population $\phi(t)$ in the potential well at $x = \delta_0$:

$$t = \tau \log \left(\frac{\phi(t) - 1/2}{\phi(0) - 1/2} \right) \left[\log \left(\text{erf} \left(\frac{1}{\sqrt{2\tau}} \right) \right) \right]^{-1}. \quad (12)$$

Beginning with $\phi(0) = 1$ and setting $\phi(t) = 0.525$ (i.e., 95% of steady state), we show the time required to achieve 95% conversion of particles as a function of the dimensionless period in Fig. 5, which also depicts the optimal period.

Thus, the simple unidimensional model mathematically establishes the existence of an optimal period of pulsing to attain the steady state, $\tau_{\text{opt}} \sim O(1)$, i.e., $T \sim \delta_0^2/D$. Given a unit duty cycle ($\eta = 1$), the model predicts that $t_{\text{Off}} \sim (\text{range})^2/D$, similar to the Brownian dynamics simulations (Section 3.1). Further, because we have assumed that the process of collecting the particles into the wells during the on portion of the cycle is instantaneous, the effect of changing the duty-cycle of the pulsing process is straightforward to incorporate into the

model. If the off fraction of the cycle is $1/(\eta + 1)$, then replacing τ with $\tau/2(\eta + 1)$ in the above expressions recovers the correct dynamics for arbitrary duty cycle.

3.3 Effect of the duty cycle

It is clear from the arguments based on scaling as well as kinetic theory that the optimal off duration is dictated by the diffusion timescale based on range of the potential. However, the discussion thus far has assumed the presence of an *a priori* nucleated particle cluster. If the suspension is sufficiently dilute, the probability of forming a critical crystalline nucleus decreases. The duty cycle of the pulsing process is the tunable parameter that governs the formation of such nuclei.

The mean inter-particle separation $\bar{\ell}$, between freely suspended Brownian particles, scales in two dimensions as $\bar{\ell} \sim \phi^{-1/2}$. On average, the particles need to diffuse across this separation to interact via the short-range attractive potential. Therefore, in order to aggregate spontaneously, the on-state of the interaction potential for a dilute suspension needs to be of the same order as the diffusion time based on the mean inter-particle sepatation, i.e., $t_{\text{On}} \sim \bar{\ell}^2/D \sim \phi^{-1} a^2/D$. It follows that the duty cycle (η) scales as,

$$\eta = t_{\text{On}}/t_{\text{Off}} \sim \phi^{-1},$$

since the optimal off duration (t_{Off}) is independent of the concentration (from Sections 3.1 and 3.2).

Fig. 6 shows that upon decreasing concentration of the suspension and keeping the off duration constant at its optimal value (D/δ_0^2), higher duty cycles are required to achieve self-assembly. Note that the scaling argument anticipates that nucleation is spontaneous. In other words, the formation of a critical nucleus is expected to be an *almost certain* event (i.e., the critical nucleus size is 1 particle). Thus, the behavior depicted in Fig. 6 is a dynamic equivalent of a thermodynamic phase diagram, wherein the ϕ^{-1} scaling plays the role of a spinodal boundary. However, it should be noted that the co-existence is a dynamical steady state, instead of a thermodynamic equilibrium, because the interaction potential varies periodically in time.

Scaling with ϕ^{-1} is a property of the dimensionality of the system. As discussed above, the scaling arises due to the square-root dependence of mean inter-particle separation on the concentration in two dimensions. In three dimensions, the mean inter-particle separation scales as the cube root of the concentration ($\bar{\ell} \sim \phi^{-1/3}$). Thus, we expect that the duty cycle required for nucleation and growth scales as inverse $2/3^{\text{rd}}$ power of the concentration ($\eta \sim \phi^{-2/3}$).
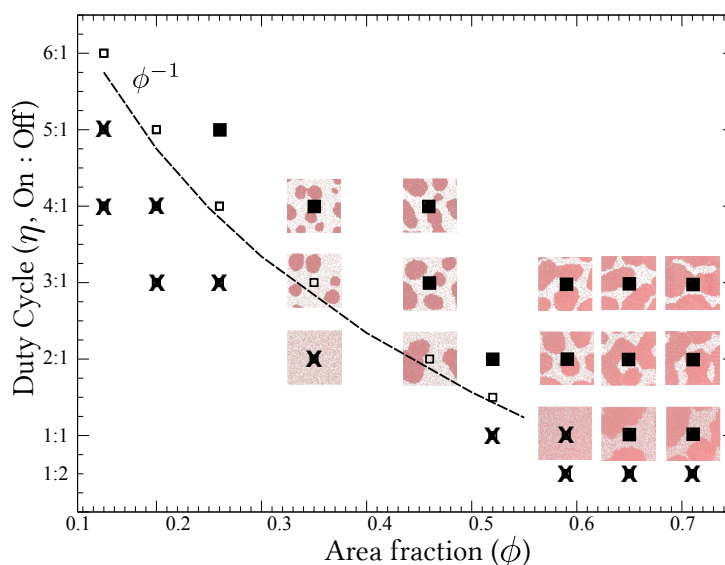
Fig. 6 Effective phase diagram for a pulsed inter-particle pair potential with a range of $0.1a$ and consequently, the duration of off-state $t_{\text{Off}} = 0.01$. Each point on the diagram represents the status of a simulated suspension after 300000 on-off cycles. Filled squares (■) indicate formation of crystals via spontaneous nucleation (nucleation starts almost immediately after a pulsed potential is applied), crosses (**X**) indicate that the suspension never exhibited nucleation, and open squares (□) depict the border-line cases in which nucleation was not instantaneous upon application of the pulsed potential.

4 Conclusions

We have demonstrated a procedure for dynamic self-assembly of colloidal crystals via 'tunable annealing' of kinetically arrested colloidal glasses, formed under the influence of a short-range attractive interaction between colloidal particles. The procedure entails periodic pulsing of the interaction between on- and off-states. We have shown that there are two independent tunable parameters involved, namely, the off duration and the duty cycle of the pulsing process. The duty cycle is the ratio of the duration of the on-state to that of the off-state. Both tunable parameters exhibit optimum values to attain crystalline state.

For a fixed duty cycle of 1, we have shown that the optimal off duration is given by the time required for a single colloidal particle to diffuse through the range of the short-range attraction ($t_{\text{Off}} \sim \text{range}^2 \times 6\pi\mu a/k_BT$). Concentrated systems with mean inter-particle separation smaller than the range of potential are used to demonstrate the above scaling. Considering a typical colloidal suspension at 300 K, comprised by particles of 2 μm diameter, if the range of short-ranged inter-particle attraction is approximately 100 nm, the aforementioned optimal off duration is approximately 0.05s. With a unit duty cycle, this translates to a pulsing frequency of 10 Hz. When the duration of the off-state is fixed to its optimal value, the duty cycle required for nucleation and growth scales inversely with the concentration of the suspension, thus giving rise to a dy-

namical 'phase boundary'. The systems used to demonstrate this scaling behavior exhibit the limiting scenario in which the mean inter-particle separation is much larger than the range of the inter-particle interaction.

The implications of employing a time-periodic potential for colloidal self-assembly are plain: it is a generic physical process independent of the nature of the applied potential, which provides tunable parameters to control and widen the envelope for self-assembly by circumventing the barriers to growing large, low defect crystalline domains. Practical feasibility of this strategy has been demostrated experimentally using suspensions of paramagnetic colloids in a pulsed magnetic field,[17] and we have demostrated here that the inferences from the present work translate well, at least qualitatively, to those experimental observations. A similar exercise can be undertaken for the case of dielectric colloids in pulsed electric fields. The general applicability of this phenomenon to chemical and biological systems will be explored by investigating systems such as colloids with temperature responsive stickers (e.g., DNA[25–27]) in periodically pulsed temperatures, such that the stickers can be molten or frozen periodically to toggle inter-particle interactions.

Appendix A: Simplification of velocity-Verlet scheme for overdamped colloidal dynamics

$$
\begin{aligned}
\mathbf{x}_i(t+\Delta t) &= \mathbf{x}_i(t) + \frac{1}{m_i}\mathbf{p}_i(t)\Delta t \\
&\quad + \frac{1}{2m_i}\left(\mathbf{F}_i(t) - \frac{\gamma_i}{m_i}\mathbf{p}_i(t-\Delta t/2)\right)\Delta t^2 \\
\mathbf{p}_i(t+\Delta t/2) &= \mathbf{p}_i(t) + \frac{1}{2}\left(\mathbf{F}_i(t) - \frac{\gamma_i}{m_i}\mathbf{p}_i(t-\Delta t/2)\right)\Delta t \\
\mathbf{p}_i(t+\Delta t) &= \mathbf{p}_i(t+\Delta t/2) \\
&\quad + \frac{1}{2}\left(\mathbf{F}_i(t+\Delta t) - \frac{\gamma_i}{m_i}\mathbf{p}_i(t+\Delta t/2)\right)\Delta t
\end{aligned}
$$

Here, $(\mathbf{x}_i, \mathbf{p}_i)$ are position and momentum of particle i in the simulation, m_i is its mass, γ_i is the corresponding drag coefficient, and $\mathbf{F}_i$ is the force acting on the particle. As mentioned in Section 2, a specific choice of particle mass ($m_i = \gamma_i\Delta t$) simplifies above equations to the exact forward-in-time Euler integration scheme for overdamped dynamics of colloids:

$$
\mathbf{x}_i(t+\Delta t) = \mathbf{x}_i + \frac{1}{\gamma_i}\mathbf{F}_i(t)\Delta t.
$$

The above forward-in-time integration represents the exact overdamped dynamics of a particle, with negligible inertia. Therefore, overdamped dynamics of colloidal particles can be simulated in HOOMD by setting particle mass proportional to the time-step. With this choice of mass, our simulation method recovers the correct overdamped dynamics of colloids.

Appendix B: Effective energy landscape in asymptotically fast pulsing

Colloidal dynamics in a general potential energy landscape is governed by the Smoluchowski equation:

$$
\frac{\partial P}{\partial t} = D\frac{\partial}{\partial \mathbf{x}}\left[\frac{\partial P}{\partial \mathbf{x}} + P\frac{\partial \beta U}{\partial \mathbf{x}}\right],
$$

where, P is the N-particle probability density, D is the diffusivity, and $\beta U = U/k_B T$ is the interaction potential normalized on thermal noise $k_B T$. The formal solution to the above Smoluchowski equation can be written as,

$$
P(\mathbf{x},t) = e^{tL}P(\mathbf{x},0).
$$

Here, L is the linear differential operator given by,

$$
L \equiv D\frac{\partial}{\partial \mathbf{x}}\left[\frac{\partial(\ldots)}{\partial \mathbf{x}} + (\ldots)\frac{\partial \beta U}{\partial \mathbf{x}}\right].
$$

In the case of a time-periodic process, such as pulsing a potential, we can relate the probability distribution at the end of a cycle to that at the end of the previous cycle using the above formal representation. Consider a pulsing process with duty cycle η and pulsing period T, such that the off and on durations of a pulsing cycle can be represented by operators L_{Off} and L_{On}, respectively, given as:

$$
L_{\text{Off}} \equiv D\frac{\partial}{\partial \mathbf{x}}\left[\frac{\partial(\ldots)}{\partial \mathbf{x}}\right], \text{ and,}
$$

$$
L_{\text{On}} \equiv D\frac{\partial}{\partial \mathbf{x}}\left[\frac{\partial(\ldots)}{\partial \mathbf{x}} + (\ldots)\frac{\partial \beta U}{\partial \mathbf{x}}\right]
$$

The distribution at the end of nth cycle in terms of that at the end of the $(n-1)^{\text{th}}$ cycle is given by,

$$
P(\mathbf{x},nT) = e^{\frac{\eta T}{\eta+1}L_{\text{On}}}e^{\frac{T}{\eta+1}L_{\text{Off}}}P(\mathbf{x},(n-1)T).
$$

In dimensionless form, the period T changes to $\tau = DT/\delta_0^2$, where δ_0 is the characteristic length associated with the potential U. In the high frequency limit, $\tau << 1$, only the leading order terms in the exponential operator suffice to describe the dynamics of pulsing. Therefore,

$$
\begin{aligned}
P(\mathbf{x},n\tau) &= e^{\frac{\eta \tau}{\eta+1}L_{\text{On}}}e^{\frac{\tau}{\eta+1}L_{\text{Off}}}P(\mathbf{x},(n-1)\tau) \\
&\approx \left[\left(1 + \frac{\eta \tau L_{\text{On}}}{\eta+1}\right)\left(1 + \frac{\tau L_{\text{Off}}}{\eta+1}\right)\right]P(\mathbf{x},(n-1)\tau)
\end{aligned}
$$

Rearranging the above equation,

$$
\begin{aligned}
\frac{1}{\tau}&\left(P(\mathbf{x},n\tau) - P(\mathbf{x},(n-1)\tau)\right) \\
&\approx \left[\frac{\eta}{\eta+1}L_{\text{On}} + \frac{1}{\eta+1}L_{\text{Off}}\right]P(\mathbf{x},(n-1)\tau)
\end{aligned}
$$

$$(13)$$

However, notice that $L_\eta = [\eta/(1+\eta)]L_{\text{On}} + [1/(1+\eta)]L_{\text{Off}}$ can be rewritten (in dimensionless form) as:

$$
L_\eta \equiv \frac{\partial}{\partial \mathbf{x}}\left[\frac{\partial(\ldots)}{\partial \mathbf{x}} + (\ldots)\frac{\eta}{\eta+1}\frac{\partial \beta U}{\partial \mathbf{x}}\right]
$$

Taking limit $\tau \to 0$ in equation 13 and using the above definition of L_η, we recover Smoluchowski equation,

$$
\frac{\partial P}{\partial \tau} = L_\eta P.
$$

This shows that in the high frequency limit, the pulsing process is equivalent to applying a steady potential rescaled by the duty fraction: $\eta/(1+\eta)$.

References

1 K. Nakayama, K. Tanabe and H. Atwater, *Appl. Phys. Lett.*, 2008, **93**, 121904.

2 X. Meng, R. Al-Salman, J. Zhao, N. Borissenko, Y. Li and F. Endres, *Angew. Chem.*, 2009, **48**, 2703–2707.

3 K. Kanamura, N. Akutagawa and K. Dokko, *J. Power Sources*, 2005, **146**, 86–89.

4 V. L. Alexeev, A. C. Sharma, A. V. Goponenko, S. Das, I. K. Lednev, C. S. Wilcox, D. N. Finegold and S. A. Asher., *J. Am. Chem. Soc.*, 2003, **75**, 2316–2323.

5 J. Schilling, R. B. Wehrspohn, A. Birner, F. Müller, R. Hillebrand, U. Gösele, S. W. Leonard, J. P. Mondia, F. Genereux, H. M. van Driel, P. Kramper, V. Sandoghdar and K. Busch, *J. Optics A*, 2001, **3**, S121–S132.

6 S. Foulger, P. Jiang, A. Lattam, D. S. Jr., J. Ballato, D. Dausch, S. Grego and B. Stoner, *Adv. Mat,*, 2003, **15**, 685–689.

7 K. D. Hermanson, S. O. Lumsdon, J. P. Williams, E. W. Kaler and O. D. Velev, *Science*, 2001, **294**, 1082–1086.

8 N. Padture, K. W. Schlichting, T. Bhatia, A. Ozturk, B. Cetegen, E. H. Jordan, M. Gell, S. Jiang, T. D. Xiao, P. R. Strutt, E. García, P. Miranzo and M. I. Osendi, *Acta Mat.*, 2001, **49**, 2251–2257.

9 M. Grzelczak, J. Vermant, E. Furst and L. Liz-Marzan, *ACS Nano*, 2010, **4**, 3591–3605.

10 A. Hynninen and M. Dijkstra, *Phys. Rev. Lett.*, 2005, **94**, 138303.

11 A. Goyal, C. K. Hall and O. D. Velev, *Phys. Rev. E*, 2008, **77**, 031401.

12 K. Bishop, C. Wilmer, S. Soh, and B. Grzybowski, *Small*, 2009, **5**, 1600–1630.

13 P. G. Vekilov, *Nanoscale*, 2010, **2**, 2346–2357.

14 P. R. ten Wolde and D. Frenkel, *Science*, 1997, **277**, 1975–1978.

15 B. Ackerson and K. Schatzel, *Phys. Rev. E*, 1995, **52**, 6448–6460.

16 P. A. Swan, J. W.and Vasquez, P. A. Whitson, E. M. Fincke, K. Wakata, S. H. Magnus, F. D. Winne, M. R. Barratt, J. H. Agui, R. D. Green, N. R. Halld, D. Y. Bohmand, C. T. Bunnelle, A. P. Gast and E. M. Furst, *Proc. Natl. Acad. Sci. U. S. A.*, 2012, **109**, 16023–16028.

17 J. W. Swan, J. L. Bauer, Y. Liu and E. M. Furst, *Soft Mat.*, 2014, **10**, 1102–1109.

18 J. A. Anderson, C. D. Lorenz and A. Travesset, *J. Comp. Phys.*, 2008, **227**, 5342–5359.

19 J. W. Swan and J. F. Brady, *Phys. Fluids*, 2007, **19**, 113306.

20 S. G. Anekal and M. A. Bevan, *J. Chem. Phys.*, 2006, **125**, 034906.

21 B. Cichocki, R. B. Jones, R. Kutteh and E. Wajnryb, *J. Chem. Phys.*, 2000, **112**, 2548–2561.

22 D. M. Heyes and J. R. Melrose, *J. Non-Newton. Fluid.*, 1993, **46**, 1–28.

23 J. F. Brady and J. F. Morris, *J. Fluid Mech.*, 1997, **348**, 103–139.

24 P. J. Lu, E. Zaccarelli, F. Ciulla, A. B. Schofield, F. Sciortino and D. A. Weitz, *Nature*, 2008, **453**, 499–504.

25 V. T. Milam, A. L. Hiddessen, J. C. Crocker, D. J. Graves and D. A. Hammer, *Langmuir*, 2003, **19**, 10317–10323.

26 D. Nykypanchuk, M. M. Maye, D. van der Lelie and O. Gang, *Nature*, 2008, **451**, 549–552.

27 J. A. Fan, H. Yu, B. Kui, W. Chihhui, B. Jiming, N. B. Schade, V. N. Manoharan, G. Shvets, P. Nordlander, D. R. Liu and F. Capasso, *Nano Lett.*, 2011, **11**, 4859–4864.
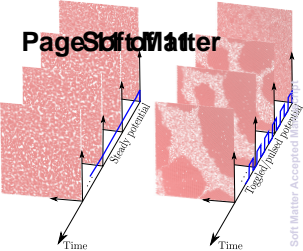
Periodic pulsing of inter-particle potential facilitates colloidal self-assembly by effectively 'tunneling' through barriers.